AGU PUBLICATIONS

Geophysical Research Letters

RESEARCH LETTER
10.1002/2014GL061068

Key Points:
- No simple relationship between the acoustic amplitude and bubble overpressure
- Below ΔP = 24 kPa, the monopole source theory holds true
- The energy computed over the first period is a good proxy for the total energy

Correspondence to:
V. Vidal,
valerie.vidal@ens-lyon.fr

Citation:
Sánchez, C., B. Álvarez, F. Melo, and V. Vidal (2014), Experimental modeling of infrasound emission from slug bursting on volcanoes, *Geophys. Res. Lett.*, *41*, 6705–6711, doi:10.1002/2014GL061068.

Received 1 JUL 2014
Accepted 9 SEP 2014
Accepted article online 14 SEP 2014
Published online 6 OCT 2014

Experimental modeling of infrasound emission from slug bursting on volcanoes

C. Sánchez[1], B. Álvarez[1], F. Melo[1], and V. Vidal[2]

[1]Laboratorio de Física No Lineal, Departamento de Física, Universidad de Santiago de Chile, Santiago, Chile, [2]Laboratoire de Physique, École Normale Supérieure de Lyon – CNRS, Université de Lyon, Lyon, France

Abstract The acoustic signal produced by gas slugs bursting at volcano vents is investigated by means of laboratory experiments. In order to explore the transition between linear and nonlinear acoustics, we model the bubble by an overpressurized cylindrical cavity closed by a membrane. We find that the acoustic waveform inside and outside the cavity, produced by the membrane bursting, is well described by the linear acoustics equations and a monopole source model up to an initial overpressure inside the cavity of about 24 kPa. For higher overpressure, the amplitude inside the conduit is smaller than the linear prediction, whereas the amplitude measured outside is larger. The frequency content remains harmonic, even at high initial overpressure. Changing the bursting depth in the conduit does not change the scaling of the amplitudes but affects the waveform and energy partitioning. We show that the energy of the first signal period is about 30% of the total acoustic energy and can be used as a good estimate, with a geometrical correction to account for the bursting depth.

1. Introduction

Strombolian activity is commonly described as the repetitive bursting of overpressurized gas bubbles as large as the volcanic conduit (slugs) [see, for instance, *Blackburn et al.*, 1976; *Jaupart and Vergniolle*, 1988; *Vergniolle and Brandeis*, 1994, 1996; *Ripepe et al.*, 2001, and references therein]. Estimating the overpressure inside the bubble before the explosion is still a major challenge. Indeed, field measurements only provide an indirect estimate of this value. The bubble overpressure may be thus quantified from direct visualization of bubble bursting [*Blackburn et al.*, 1976; *Wilson*, 1980; *Taddeucci et al.*, 2012] or inversion models of the acoustic waveform, which consider either a resonant volcanic conduit [*Buckingham and Garcés*, 1996; *Garces et al.*, 2000; *Hagerty et al.*, 2000], vibration of the bubble before its bursting [*Vergniolle and Brandeis*, 1994, 1996; *Vergniolle et al.*, 1996], or gas overpressure release at bursting [*Lane et al.*, 2013]. This quantification, however, would strongly help to understand the eruption behavior and further constrain the seismoacoustic models.

Previous estimates of the overpressure inside the bubble before its explosion strongly vary, from 25 kPa for Heimaey, Iceland [*Blackburn et al.*, 1976], 600 Pa [*Blackburn et al.*, 1976], to 0.1–0.5 MPa for Stromboli [*Vergniolle and Brandeis*, 1996; *Taddeucci et al.*, 2012], between 0.08 and 1.4 MPa for Shishaldin volcano [*Vergniolle et al.*, 2004], to 3.4 MPa for Arenal volcano [*Hagerty et al.*, 2000]. The large range of overpressure estimates, from a few kPa up to several MPa [*Gonnermann and Manga*, 2007], makes it difficult to assess in which regime the acoustic problem has to be considered. Several radiation models of infrasonic waves have pointed out that depending on the complexity of the sound variations, a volcano may be considered as a monopole, dipole, or even quadrupole source [*Johnson et al.*, 2008]. These models, however, have often been developed in the linear acoustic regime, where the wave amplitude should be much smaller than the atmospheric pressure. What happens then if entering a nonlinear regime?

Based on laboratory experiments, we investigate the acoustic wave produced by the overpressure release of a cylindrical cavity initially closed by a membrane. The setup is analogous to a slug bursting in an open conduit volcano, such as Stromboli, for instance [*Ripepe et al.*, 2007]. This configuration makes it possible not only to control the overpressure before bursting but also to explore the transition between the linear and nonlinear acoustic regimes. Finally, by adding an extra conduit length on top of the system, we investigate the effect of the bubble bursting depth in the conduit on the acoustic waveform.

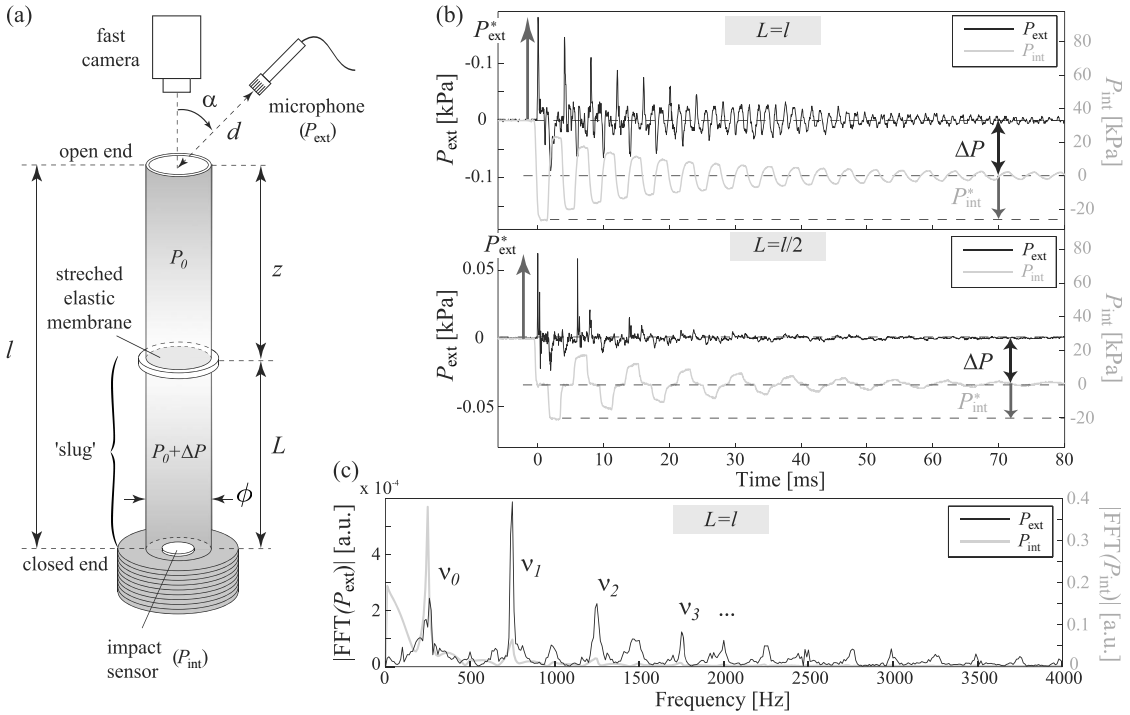

Figure 1. (a) Experimental setup. We impose an overpressure ΔP inside a cylindrical cavity closed by a membrane located at a distance L from the cavity bottom. When the membrane bursts, the acoustic signal is recorded inside, P_{int}, and outside, P_{ext}, the cavity. (b) Amplitude of the acoustic wave recorded inside (P_{int}, gray line) and outside (P_{ext}, black line) the cavity after bursting. ((top) $L = l = 32$ cm; (bottom) $l = 64$ cm, $L = l/2$; $\Delta P \simeq 30$ kPa). (c) Spectrum of the acoustic waveform inside (gray line) and outside (black line) the cavity, for the signals displayed in Figure 1b (top).

2. Experimental Setup

The experimental setup consists of a cylindrical cavity (length $l = 0.16$ to 0.64 m, inner diameter $\phi = 25.4$ mm) drilled in plexiglas (Figure 1a). The tube is closed at the bottom end (rigid bottom). An elastic membrane (latex, thickness $e = 0.5$ mm) is initially stretched over a ring and located at a height $L \leq l$ inside the tube. Air is then injected in the lower part of the cavity, up to a controlled overpressure ΔP, which can be varied from 0 to a 0.8 bar. The topmost end of the tube (at height l) remains open.

At time $t = 0$ a needle, fixed on a motorized arm, pierces the center of the elastic membrane, which ruptures suddenly. Previous experiments have pointed out that in the linear regime, the wave amplitude may be strongly reduced when the typical bubble rupture time, τ_{rupt}, becomes comparable to, or larger than, the wave propagation time in the cavity, $\tau_{prop} = 2l/c$, where c is the sound speed [*Vidal et al.*, 2006, 2010]. We recorded the membrane aperture dynamics with a fast camera (Phantom v9.1, up to 23000 frames per second). In all our experiments, the rupture time $\tau_{rupt} \leq 0.2$ ms is always smaller than the typical propagation time of the wave inside the cavity, τ_{prop}, whichever the position of the membrane in the tube (from $l = 0.16$ m to $l = 0.64$ m, $\tau_{prop} \simeq 0.9$ to 3.8 ms, respectively). This configuration makes it possible to neglect the effect of the membrane aperture dynamics on the acoustic wave amplitude. In the following, we can therefore consider that the opening is instantaneous.

The acoustic wave produced by the membrane bursting is monitored outside the tube by a microphone (PCB Piezotronics Inc., 1/4" microphone 377A10 + preamplifier 426B03). The microphone is located at a distance d from the cavity aperture (typically $d \simeq 1$ m), at an angle $\alpha = 45°$ from the vertical . The acoustic waveform does not change much when varying α from 0 to 90°. We do not position the microphone at the vertical of the tube to avoid the signal generated by air advection during the overpressure release, which is not an acoustic wave. Simultaneously, we measure the pressure signal at the bottom of the cavity with an impact sensor (Force sensor PCB Piezotronics PCB 200B02 + amplifier PCB 482A16). Both signals are recorded by means of two oscilloscopes (Tektronix TDS2012B, sampling frequency 25 kHz).

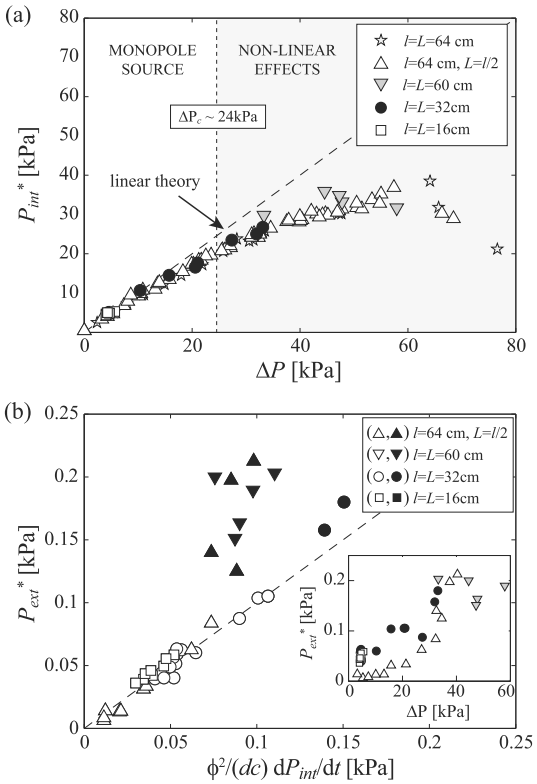

Figure 2. (a) Maximum amplitude of the acoustic waveform inside the cavity, P^*_{int}, as a function of ΔP (dashed line: linear theory). The monopole source approximation remains valid up to $\Delta P_c \simeq 24$ kPa (from Figure 2b, see text). Significant nonlinear effects are observed when $\Delta P > \Delta P_c$. (b) Maximum amplitude of the acoustic waveform outside the cavity, P^*_{ext}, as a function of the excess pressure predicted by Lighthill's monopole source theory (see text) (white symbols, $\Delta P \leq \Delta P_c$; black symbols, $\Delta P > \Delta P_c$; dashed line: Lighthill's theory). Inset: P^*_{ext} versus ΔP does not display any obvious relation.

3. The Acoustic Waveform

Figure 1b displays the acoustic waveforms inside (P_{int}, gray line) and outside (P_{ext}, black line) the cavity for different membrane positions in the tube. Here we point out the example of a "slug" of the same volume ($L = 32$ cm) and initial overpressure ($\Delta P \simeq 30$ kPa) bursting either at the top of the conduit ($l = L$, Figure 1b, top) or at half the conduit length ($l = 2L$, Figure 1b, bottom). At bursting, P_{int} initially drops from ΔP to $-P^*_{\text{int}}$. The signal inside the cavity is then resonant, the wave traveling back and forth in the cavity, and damps over a few tens of milliseconds. When the membrane bursts at depth in the cavity (Figure 1b, bottom), we clearly note that the wave front is double, due to both an upward positive pressure front and a downward negative pressure front traveling in the cavity. The outside pressure (P_{ext}, black line) shows different successive peaks, in phase with each change of the wave amplitude inside. We note P^*_{int} (resp. P^*_{ext}) the amplitude of the first peak of the excess pressure inside (respectively, outside) the cavity, which is higher than that of any successive peaks.

3.1. Amplitude

In the linear acoustic regime, due to the condition of total reflection at the cavity bottom, the pressure amplitude in the cavity, P^*_{int}, is strictly equal to the initial overpressure in the cavity before bursting, $P^*_{\text{int}} = \Delta P$. To investigate the transition toward nonlinear regimes, we report for different initial overpressure ΔP the excess pressure amplitude in the cavity, P^*_{int} (Figure 2a). We check that for different experimental configurations (different tube length l and position of the membrane in the cavity, L), the linear regime $P^*_{\text{int}} = \Delta P$ holds true up to an overpressure ΔP_c slightly higher than 20 kPa. For $\Delta P > \Delta P_c$ the excess pressure amplitude in the cavity is less than the one predicted by the linear theory, and significant nonlinear effects are observed. In the next paragraph, we propose an exact determination of the threshold overpressure ΔP_c.

The variation of P^*_{ext}, the first excess pressure peak measured outside, as a function of ΔP does not have a clear interpretation at first sight (Figure 2b, inset). To further explain the data, a model is required. Here we test the monopole source theory proposed by *Lighthill* [1978]: in the linear theory of sound, the excess pressure for a simple (point) source is given by

$$P - P_0 = \frac{\dot{q}(t - r/c)}{4\pi r}, \tag{1}$$

where P_0 denotes the atmospheric pressure, r the distance from the source, $q = \rho dV/dt$ the rate of mass outflow, with ρ the gas density and V the gas volume, and c the sound speed. For the cylindrical geometry of our experimental setup, equation (1) can be written as a function of our parameters:

$$P_{\text{ext}} = \frac{\phi^2}{16dc}\frac{dP_{\text{int}}}{dt}. \tag{2}$$

The excess pressure outside should therefore be proportional to the first derivative of the excess pressure inside the cavity. It can be qualitatively observed in Figure 1b, for example, where each pressure drop in the

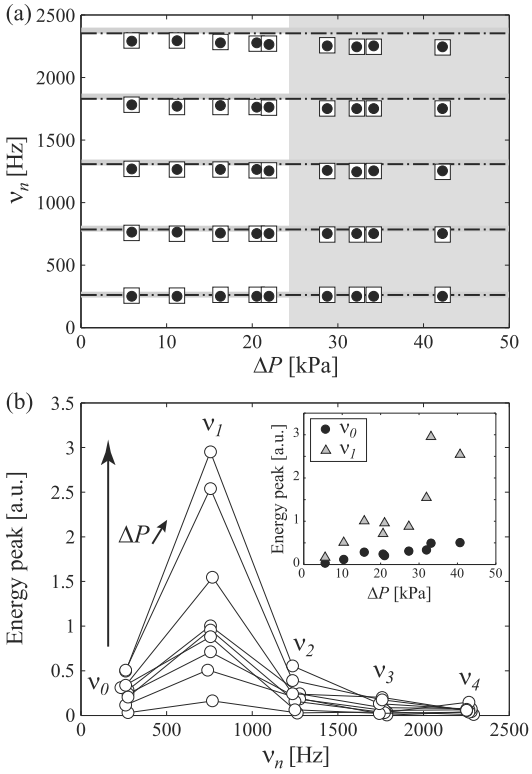

Figure 3. (a) Spectral content (peak frequencies ν_n) for P_{int} (black dots) and P_{ext} (white squares) for different ΔP compared to the theoretical harmonics of a resonant wave in the cavity (unflanged, dash-dotted lines; flanged, thick gray lines). The spectral content remains unchanged, even after the transition to nonlinear regimes (gray zone) ($L = l = 32$ cm). (b) Energy of the frequency peaks (see Figure 1c) for the first five harmonics, when ΔP increases (a.u. = arbitrary units). *Inset:* Energy of the fundamental (black dots) and the second harmonics (gray triangle) as a function of ΔP.

conduit corresponds to a sharp pressure peak outside. We find that the monopole source approximation works well up to an initial overpressure $\Delta P_c \simeq 24$ kPa (white symbols, Figure 2b), without any adjustable parameters. For $\Delta P > \Delta P_c$ the excess pressure recorded by the outside microphone is larger than the linear prediction (black symbols, Figure 2b).

Note that the bursting depth plays an important role on the amplitude. When the slug bursts at a depth $z = l - L$ in the conduit, the inner pressure derivative, dP_{int}/dt, has to be corrected by a geometrical factor $L/(L + z)$, to consider the equivalent monopole source at the conduit vent. Only after this correction do the data collapse on Lighthill's prediction in the linear regime (white triangles, Figure 2b).

3.2. Frequency Content

In the linear acoustic regime, it has been shown that for small initial overpressure, the sudden release of a pressurized cavity leads to longitudinal resonant waves in the tube, and their subsequent radiation outside [*Vidal et al.*, 2006]. The inside and outside acoustic signals are thus harmonic, with regular peaks in the spectrum given by the cavity length, $\nu_0 = c/4(l + \delta l)$ for the fundamental frequency and $\nu_n = (2n + 1)\nu_0$ for the harmonics, where c is the sound speed in air. Only the odd harmonics are present in the signal, due to the asymmetric conditions of the cavity (open top, closed bottom). Although we investigate the transition toward the nonlinear regime, all the experiments stand either in the linear sound wave or in the weak shock wave regime. The wave speed thus equals the sound speed in air ($c \simeq 346$ m/s at 25°C). δl denotes a correction length due to the radiation of the wave outside: $\delta l = 4\phi/3\pi$ (respectively, 0.3ϕ) for a flanged (respectively, unflanged) aperture [*Kinsler et al.*, 1982].

From the signal spectrum inside and outside the conduit (see Figure 1c), we can report the harmonic peak frequencies, compared with the theoretical predictions for a flanged (respectively, unflanged) aperture (Figure 3a). Previous studies of infrasonic tremor on Kilauea [*Fee et al.*, 2010] and Villarrica [*Goto and Johnson*, 2011] have linked the dominant tremor peak to Helmholtz oscillations of the cavity above the magma level in the conduit. In our experiments, however, the dominant frequency always corresponds to the fundamental mode of longitudinal resonant waves, even when the membrane bursts inside the conduit. We observe a slight decrease of the higher harmonics frequency for high ΔP, but no transition is visible through all the range of explored overpressures, even when nonlinear effects start affecting the amplitudes (gray zone).

Although the nonlinearities do not affect the harmonic frequencies, they have a strong signature on the spectral amplitudes. The signal outside bears more energy in the second harmonic, $\nu_1 = 3\nu_0$, than in the fundamental (higher peak in the spectrum). Even frequencies, $\nu_{2n} = (2n)\nu_0$, can also be observed in the spectrum (Figure 1c), resulting from nonlinear coupling and energy transfer to higher modes.

3.3. Acoustic Energy

In this section, we consider the total energy of the acoustic signal measured outside the cavity, defined by

$$E_a = \frac{2\pi d^2}{\rho c} \int_0^\infty P_{\text{ext}}^2 \, dt \tag{3}$$

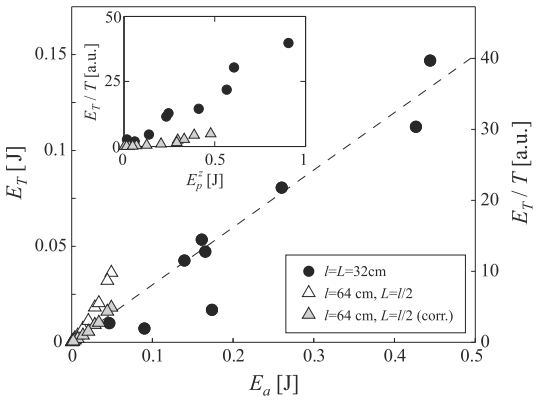

Figure 4. Energy E_T of the first signal period outside (P_{ext}) as a function of the total energy of the same signal, E_a (right axis, E_T/T, gray triangles; the dashed line is a guide for the eye). *Inset:* E_T/T as a function of the potential energy initially stored in the slug, corrected by the bursting depth z (a.u. = arbitrary units).

for a half-space radiation. It is often difficult to accurately estimate E_a. Indeed, the signal recorded in the field can result from the superposition of acoustic waveforms generated by successive burstings, and estimating the end of the sound emitted by a single bursting may be impossible. We propose to compare the total energy, E_a, to the energy of the same signal, computed over the first signal period only:

$$E_T = \frac{2\pi d^2}{\rho c} \int_0^T P_{\text{ext}}^2 \, \mathrm{d}t. \tag{4}$$

Figure 4 shows that E_T is a good proxy for the estimation of the acoustic energy. However, in order to compare this parameter for slugs bursting at different depths (here $z = 0$, black dots versus $z = L$, white triangles), it is necessary to consider E_T/T, where $T = 1/\nu_0$ is the period of the fundamental. This parameter takes into account the change in wavelength due to wave resonance in different conduit lengths. After correction (gray triangles, Figure 4), all data follow the same trend. Note that the energy of the first signal period is about 30% the total acoustic energy.

In Figure 4, inset, we compare E_T/T to the potential energy E_p initially stored in the slug before bursting. E_p can be evaluated by considering the adiabatic expansion of the gas volume $V = \pi(\Phi/2)^2 L$ (slug volume, Figure 1a) when the membrane bursts:

$$E_p = \frac{1}{2} \frac{V \Delta P^2}{\rho c^2}. \tag{5}$$

For a slug bursting at depth z, the effective potential energy corresponding to the whole resonating conduit is $E_p^z = E_p/(1 + z/L)$. The energy measured outside increases as the potential energy increases, as expected. However, although all corrections are taken into account (period of the signal and geometry of the conduit), there is still a difference when the slug bursts at the top or inside the conduit.

Energy losses are mainly governed by viscous dissipation along the cavity walls and radiation of the wave at the vent. In the linear acoustic regime, the characteristic wave damping time associated with these processes, τ_n^v and τ_n^Z, respectively, can be determined analytically for the n^{th} harmonic (frequency ν_n) [*Vidal et al.*, 2006]: $\tau_n^v = \phi/\sqrt{4\pi\nu_n\eta^*}$ where $\eta^* = \eta[1 + (\gamma - 1)P_r^{1/2}]$ accounts for the thermal loss at the wall, with $\eta = 1.5 \times 10^{-5}$ m^2 s^{-1} the air kinematic viscosity, $P_r \simeq 0.7$ the Prandtl number, and $\gamma = 1.4$ the specific heat ratio; and $\tau_n^Z = (c/\pi\phi)^2(2n + 1)/(2\nu_n^3)$. Note that the damping due to viscous dissipation dominates at low frequencies, while the damping due to radiation dominates at high frequencies. We thus expect the radiation (respectively, viscous dissipation) to be the dominant regime for short (respectively, long) tubes. The conduit length l_c for which both processes are of the same order of magnitude is found by solving $\tau_n^v = \tau_n^Z$, with $\nu_n = (2n + 1)c/4l_c$ ($\delta l \ll l_c$):

$$l_c(n) = \left(\frac{\Phi^3}{32}\right)^{2/5} \left(\frac{c}{\eta^*}\right)^{1/5} \pi^{3/5}(2n + 1)^{3/5}. \tag{6}$$

For the parameters of our experiments, radiation (respectively, viscous dissipation) is the dominant process for the conduit length $l = 32$ cm (respectively, $l = 64$ cm), which could explain the difference in the acoustic energy (Figure 4, inset).

4. Concluding Remarks

One of the key points in field data analysis is the information which can be extracted from the acoustic signal monitored on volcanoes, P_{ext}. We have shown here that a harmonic spectrum is the signature of resonant modes in the conduit produced by bubble bursting, even when nonlinear effects become significant. The

dominant frequency is fixed by the total conduit length and, rescaled to volcanoes, lays in the infrasound range. The amplitude of the first pressure peak outside, P^*_{ext}, is well described by a monopole source theory for $\Delta P < \Delta P_c \simeq 24$ kPa. This empirical threshold holds true for different conduit lengths and bubble bursting depths. At present, no model was found to account for this value. However, it is expected to hold true for the volcanic scenario, as long as resonant waves are generated by slug bursting on the conduit. For $\Delta P > \Delta P_c$, strong departures are observed from the linear prediction and it is not possible to infer the initial bubble overpressure, ΔP, from the excess pressure amplitude—even in a well-controlled experiment.

Strombolian explosions occur on a complex spectrum of dynamics. Although slug expansion and bursting is often invoked as the source mechanism, recent observations have reported the existence of blast waves at the onset of the explosion, and supersonic jet at the origin of the infrasound [*Matoza et al.*, 2009; *Marchetti et al.*, 2013; *Taddeucci et al.*, 2014]. Our experiment investigates the transition between linear and nonlinear acoustics but does not extend to the highly nonlinear, supersonic, strong shock wave regime. The results are transposable to volcano data analysis in the limit of weak shock waves, for simple and impulsive explosions due to slug bursting. In the field, moreover, additional effects should be taken into account, for instance, the bubble rupture time, which has been pointed out as responsible for a drastic decrease of the acoustic wave amplitude, or temperature gradients.

We propose that the energy computed over the first signal period, E_T, is a good proxy for the total acoustic energy, E_a. This can be useful when successive burstings occur, and their acoustic signatures overlap. E_T/E_a is constant and of about 30% when the bursting occurs at the vent, and more when bursting at depth. For a constant gas outflux and slugs of similar length and overpressure, the slope between E_T and E_a provides a direct indication of the bursting depth, i.e., of the magma level in the conduit.

Acknowledgments

The data sets used in this article are available and can be provided by the corresponding author upon request (valerie.vidal@ens-lyon.fr). "The authors acknowledge financial support CONICYT 21110609". We thank J.-C. Géminard for fruitful discussions, and three anonymous reviewers who greatly helped us improving the manuscript.

Andrew Newman thanks three anonymous reviewers for their assistance in evaluating this paper.

References

Blackburn, E., L. Wilson, and R. Sparks (1976), Mechanics and dynamics of Strombolian activity, *J. Geol. Soc. London*, *132*, 429–440.

Buckingham, M. J., and M. A. Garcés (1996), Canonical model of volcano acoustics, *J. Geophys. Res.*, *101*(B4), 8129–8151.

Fee, D., M. Garcés, M. Patrick, B. Chouet, P. Dawson, and D. Swanson (2010), Infrasonic harmonic tremor and degassing bursts from Halema'uma'u Crater, Kilauea Volcano, Hawaii, *J. Geophys. Res.*, *115*, B11316, doi:10.1029/2010JB007642.

Garces, M., S. McNutt, R. Hansen, and J. Eichelberger (2000), Application of wave-theoretical seismoacoustic models to the interpretation of explosion and eruption tremor signals radiated by Pavlof volcano, Alaska, *J. Geophys. Res.*, *105*, 3039–3058.

Gonnermann, H. M., and M. Manga (2007), The fluid mechanics inside a volcano, *Annu. Rev. Fluid Mech.*, *39*, 321–356.

Goto, A., and J. B. Johnson (2011), Monotonic infrasound and Helmholtz resonance at Volcan Villarrica (Chile), *Geophys. Res. Lett.*, *38*, L06301, doi:10.1029/2011GL046858.

Hagerty, M., S. Schwartz, M. Garcés, and M. Protti (2000), Analysis of seismic and acoustic observations at Arenal Volcano, Costa Rica, 1995–1997, *J. Volcanol. Geotherm. Res.*, *101*, 27–65.

Jaupart, C., and S. Vergniolle (1988), Laboratory models of Hawaiian and Strombolian eruptions, *Nature*, *331*, 58–60.

Johnson, J. B., R. Aster, K. R. Jones, P. Kyle, and B. McIntosh (2008), Acoustic source characterization of impulsive Strombolian eruptions from the Mount Erebus lava lake, *J. Volcanol. Geotherm. Res.*, *177*, 673–686.

Kinsler, L. E., A. R. Frey, A. B. Coppens, and J. V. Sanders (1982), *Fundamentals of Acoustics,* 3rd ed., John Wiley, New York.

Lane, S. J., M. R. James, and S. B. Corder (2013), Volcano infrasonic signals and magma degassing: First-order experimental insights and application to Stromboli, *Earth Planet. Sci. Lett.*, *377–378*, 169–179.

Lighthill, J. (1978), *Waves in Fluids*, p. 504, Cambridge Univ. Press, Cambridge, U. K.

Matoza, R. S., D. Fee, M. A. Garcés, J. M. Seiner, P A. Ramón, and M. A. H. Hedlin (2009), Infrasonic jet noise from volcanic eruptions, *Geophys. Res. Lett.*, *36*, L08303, doi:10.1029/2008GL036486.

Marchetti, E., M. Ripepe, D. Delle Donne, R. Genco, A. Finizola, and E. Garaebiti (2013), Blast waves from violent explosive activity at Yasur Volcano, Vanuatu, *Geophys. Res. Lett.*, *40*, 5838–5843, doi:10.1002/2013GL057900.

Ripepe, M., S. Ciliberto, and M. D. Schiava (2001), Time constraints for modelling source dynamics of volcanic explosions at Stromboli, *J. Geophys. Res.*, *106*(B5), 8713–8727.

Ripepe, M., E. Marchetti, and G. Ulivieri (2007), Infrasonic monitoring at Stromboli volcano during the 2003 effusive eruption: Insights on the explosive and degassing process of an open conduit system, *J. Geophys. Res.*, *112*, B09207, doi:10.1029/2006JB004613.

Taddeucci, J., M. A. Alatorre-Ibargüengoitia, M. Moroni, L. Tornetta, A. Capponi, P. Scarlato, D. B. Dingwell, and D. De Rita (2012), Physical parameterization of Strombolian eruptions via experimentally-validated modeling of high-speed observations, *Geophys. Res. Lett.*, *39*, L16306, doi:10.1029/2012GL052772.

Taddeucci, J., J. Sesterhenn, P. Scarlato, K. Stampka, E. Del Bello, J. J. Pena Fernandez, and D. Gaudin (2014), High-speed imaging, acoustic features, and aeroacoustic computations of jet noise from Strombolian (and Vulcanian) explosions, *Geophys. Res. Lett.*, *41*, 3096–3102, doi:10.1002/2014GL059925.

Vergniolle, S., and G. Brandeis (1994), Origin of the sound generated by Strombolian explosions, *Geophys. Res. Lett.*, *21*(18), 1959–1962.

Vergniolle, S., and G. Brandeis (1996), Strombolian explosions. 1. A large bubble breaking at the surface of a lava column as a source of sound, *J. Geophys. Res.*, *101*(B9), 20,433–20,447.

Vergniolle, S., G. Brandeis, and J.-C. Mareschal (1996), Strombolian explosions. 2. Eruption dynamics determined from acoustic measurements, *J. Geophys. Res.*, *101*(B9), 20,449–20,466.

Vergniolle, S., M. Boichu, and J. Caplan-Auerbach (2004), Acoustic measurements of the 1999 basaltic eruption of Shishaldin volcano, Alaska: 1. Origin of Strombolian activity, *J. Volcanol. Geotherm. Res.*, *137*, 109–134.

Vidal, V., J.-C. Géminard, T. Divoux, and F. Melo (2006), Acoustic signal associated with the bursting of a soap film which initially closes an overpressurized cavity. Experiment and theory, *Eur. Phys. J. B*, *54*, 321–339.
Vidal, V., M. Ripepe, T. Divoux, D. Legrand, J.-C. Géminard, and F. Melo (2010), Dynamics of soap bubble bursting and its implications to volcano acoustics, *Geophys. Res. Lett.*, *37*, L07302, doi:10.1029/2009GL042360.
Wilson, L. (1980), Relationships between pressure, volatile content and ejecta velocity, *J. Volcanol. Geotherm. Res.*, *8*, 297–313.